Determining the Boundary of Molten Electrolyte and Aluminum in Electrolytic Cells by Detecting Their Vertical Distribution of Potential

CHANG Liming[1], ZHANG Zhaohui[1], ZHAO Xiaoyan[1], BIAN Xinxiao[1], ZUO Zengyang[2], LU Hui[3], LAO Dabao[2]

(1. *Beijing Industrial Spectral Imaging Engineering Research Center, School of Automation and Electrical Engineering*, *University of Science and Technology Beijing, Beijing* 100083; 2. *Shunde Innovation School*, *University of Science and Technology Beijing*, *Foshan* 528000; 3. *Guiyang Aluminum and Magnesium Design Institute Co Ltd*, *Guiyang* 550000)

Abstract: Aluminum production is a high energy consumption process so that maintaining fundamental compositions in balance and optimal conditions are essential. The molten electrolyte and melted aluminum are primary materials and their boundary needs to be monitored from time to time. An automatic measurement technic is presented in the paper to substitute for the traditional manual measurement work that is dull, poor efficiency and dangerous for operators. The boundary forming mechanism is analyzed, the vertical profile of electric potential is simulated, an automatic instrument is developed to sense the potential distribution, and a strategy is provided to identify the boundary according to the potential curves. Finally, some practical results are compared with manual measurements, which shows good consistency.

Keywords: Aluminum Electrolytic Cell, Boundary of Molten Materials, Electric Potential Distribution, Measurement Online

1 Introduction

The production of aluminum via electrolysis is a highly energy-consuming and carbon-emitting process. The production of one ton of aluminum requires 13,500kwh of electricity and discharges about 10 tons of CO_2.Therefore, an optimal and efficient balance state is an essential consideration, which depends on the process parameters in time.

The boundary of the liquefied aluminum and electrolyte is a fundamental parameter which directly reflect the current production status of the electrolytic cell. The electrolyte is used to maintain the electrochemical reaction and stabilize the heat balance in the cell. The liquefied aluminum is the carrier to stabilize the magnetic field, protect the cathode from oxidation. But in most of factories, the boundary is measured with a F-shape steel rod by operators. The operator inserts the rod into the electrolytic cell, lifts it up after a moment, gazes the color fading, and find the ambiguous boundary according to the different colors. That's a dull and dangerous operation. Hence, an automatic measurement technic is represented in the paper.

In this paper, an automatic measurement technic is represented. The electrolytic cell is modeled in 3D and the electric field is simulated. Since the electrical conductivity of air-electrolyte-aluminum is different and the position of the boundary is related to the change of electrical potential. A method is proposed to determine the boundary based on the electrical potential distribution. Results are good, which are comparable to the manual measurement. This way, it can help to automate the measurement of electrolyte and aluminum boundaries in the electrolytic cell, thus reducing carbon emissions and improving energy efficiency.

2 The Electrolysis Process and the Boundary Formation

2.1 The Principle of Aluminum Electrolysis

To extract aluminum from alumina, the ore should be melted and then be electrolyzed in liquid phase under huge electric currents. Due to the extremely high melting point of alumina, 2054°C, the melting process is too difficult to be economical. Until 1886, when American Hall and French Héroult each independently invented the method of aluminum refining by electrolysis of cryolite and alumina molten salt, which opened the aluminum electrolysis industry. In Hall-Héroult's aluminum electrolysis process, the raw material alumina is mixed with corrosive Na_3AlF_6, which can be melted into electrolyte just at 950°C. Then, carbon material is used as the anode and cathode, and under the action of thousands of amperes in direct current, the anode participates in electrochemical reaction and the cathode precipitates aluminum.

Fig.1 shows the structure of an electrolytic cell briefly, which consists of carbon anode and cathode bars with about 4V differential potential. The huge anode current goes through the high temperature ice crystal in molten state, leads to reduce reactions represented by the formula 2.1:

$$\frac{1}{2}Al_2O_3(dissolved)+\frac{3}{4}xC(s)=Al(l)+\frac{3}{4}\left(2-\frac{1}{x}\right)CO_2(g)+\frac{3}{2}\left(\frac{1}{x}-1\right)CO(g) \quad (2.1)$$

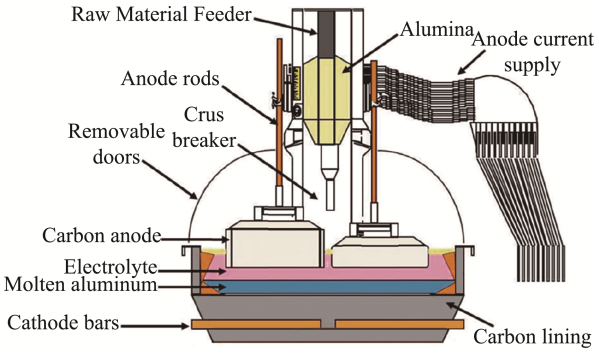

Fig.1 Brief Structure of Aluminum Electrolytic Cell

2.2 Molten Electrolyte and Aluminum Delamination Mechanism

Under the electrochemical reaction, the molten aluminum is electrolyzed above the carbon lining. At 1000°C, the density of molten cryolite is 2.095 g/cm^3 and aluminum is 2.289 g/cm^3. Hence, gravity separation will occur and will reduce the reoxidation of the aluminum by the CO_2 gas formed on the anode surfaces.

As shown in Fig.2, in the carbon anode area, due to the anodic reaction:

$$\frac{1}{2}Al_2O_3(dissolved)+\frac{3}{2}\mathrm{C(solid)}=\mathrm{Al(l)}+\frac{3}{2}CO(gas) \quad (2.2)$$

$$\frac{1}{2}Al_2O_3(dissolved)+\frac{3}{4}\mathrm{C(solid)}=\mathrm{Al(l)}+\frac{3}{4}CO_2(gas) \quad (2.3)$$

As the reaction proceeds, more electroactive substances are consumed below and to the side of the anode carbon block where CO_2 and CO gas are generated. The gas will adhere under the carbon block, producing a concentration gradient with convection. The aluminum liquid generated by the electrochemical reaction is deposited to the cathode carbon lining by convection, under the influence of gravity.

The boundary of electrolyte and aluminum can't be flat in the actual operation. Because the magneto-hydrodynamics forces are generated in the aluminum metal caused by the interaction between the magnetic fields produced by the passage of high-amperage DC electrical current through nearby conductor bars and

the electrical current flow in the aluminum metal in electrolysis cells. The large electric currents, 300–500 kA, pass through the electrically conducting liquids and generate powerful magnetic fields in the electrolytic cell. These strong magnetohydrodynamics forces increase metal velocity, metal wave height and frequency, and distortion of the aluminum–electrolyte boundary.

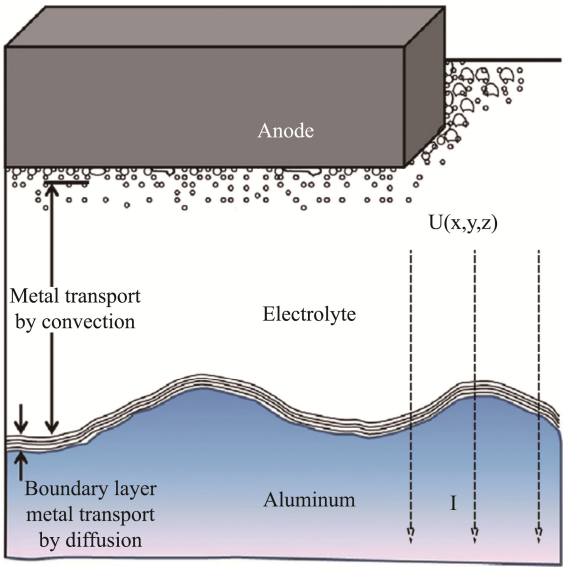

Fig.2 Formation of the Boundary [4]

3 Potential Distribution Simulation

3.1 Electrical Conductivity of Molten Cryolite and Their Mixtures

Wang[2] have measured the conductivity of mixtures obtained by adding ALF_3, AL_2O_3、CaF_2、MgF_2 and LiF to molten cryolite. Based on measurement results, the multiple regression equation for the conductivity of the cryolite melt system was obtained. The composition of the cryolite electrolyte used by Wang[2] for the determination of conductivity is shown in Table 1.

The melting point of cryolite electrolyte fluctuates in the range of 900 to 1000°C. Its conductivity data is described by the regression equation as follows:

$$ln\kappa = 1.9105 + 0.1620 \cdot CR - 17.38 \times 10^{-3}\omega(AL_3O_3) - 3.955 \times 10^{-3}\omega(CaF_2) - 9.227 \times 10^{-3}\omega(MgF_2) + 21.55 \times 10^{-3}\omega(LiF) - 1.7457 \times 10^3 T \quad (3.1)$$

κ is the conductivity, $\Omega^{-1}cm^{-1}$; ω is the mass fraction of the mixture additive, %; CR is the NaF/ALF_3 molar ratio; T is the temperature, K; The standard error of $ln\kappa$ in equation (3.1) is ± 0.0232.

Table 1 Composition of Cryolite Electrolytes Determined by Wang[2]

Composition	Scope/%	Range of changes/%
n(NaF)/n(ALF_3)	2.2~2.9	2.20,2.55,2.90
AL_2O_3	0~60	0,3.0,6.0
CaF_2	0~8.0	0,4.0,8.0
MgF_2	0~8.0	0,4.0,8.0
LiF	0~8.0	0,4.0,8.0

According to the above equation combined with the conclusions of Híveš et al[3], the conductivity of the electrolyte at 1000°C is about $2.5\,\Omega^{-1}cm^{-1}$. However, the conductivity of molten aluminum solution is not lower than that of pure aluminum due to its use as a phase state of aluminum and enhanced movement of freely movable electrons within aluminum at 1000°C. At 20°C, the conductivity of aluminum is $3.77\times10^9\Omega^{-1}cm^{-1}$, in contrast to the electrolyte at 1000°C, which is no greater than $3.0\Omega^{-1}cm^{-1}$. There is a difference of nine orders of magnitude in the conductivity of these two substances. This huge disparity gives us the theoretical basis for the measurement.

3.2 Simulation Results

The electric field in aluminum reduc-tion cell, including the electric field gener-ated by conductor current, belongs to static electric field. Laplace equation is used to describe the conductive part of aluminum reduction cell, seeing Fig.2.

$$\sigma_x \frac{\partial^2 U}{\partial^2 x^2} + \sigma_y \frac{\partial^2 U}{\partial^2 y^2} + \sigma_z \frac{\partial^2 U}{\partial^2 z^2} = 0 \quad (3.2)$$

$$\sum U = \sum I \cdot R \quad (3.3)$$

U-electric potential,

I-current,

R-resistance,

$\sigma_x, \sigma_y, \sigma_z$-conductivity in the direction of x, y and z.

Here some assumptions are given as following.

(1) The end of the steel bar embedded in the cathode carbon block is taken as the reference point, and the aluminum liquid is regarded as equipotential in the aluminum liquid layer due to the high conductivity.

(2) The cell wall and its surroundings are not conductive, and the current flows out of the cathode carbon block after passing through the electrolyte and aluminum liquid.

(3) The electrolyte properties are uniform in the whole cell.

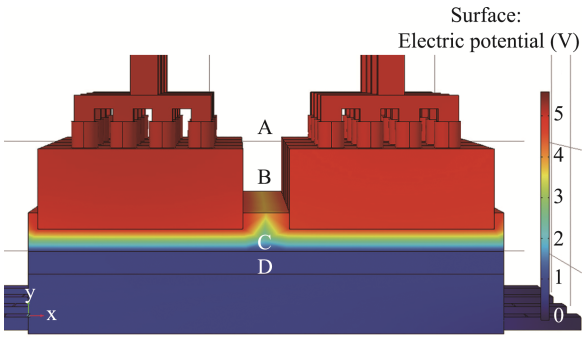

Fig.3 The Simulated Potential Distribution All over the Cell

In 3D modeling, the fluctuation of electrolyte and aluminum have been ignored. The main parts include anode rod, carbon anode, electrolyte, aluminum, carbon lining and cathode bars. In the simulation, we select the conductivity and relative permittivity of anode rod, electrolyte, aluminum liquid, carbon block, etc. The conductivity of electrolyte is less than $3.0\Omega^{-1} \cdot cm^{-1}$ according to the previous section, and here we select it to be $2.0\Omega^{-1} \cdot cm^{-1}$ at high temperature. The conductivity of aluminum liquid is taken as $3.77 \times 10^9\Omega^{-1} \cdot cm^{-1}$, and the carbon anode potential is set to be 5V. The simulation result is shown in Fig.3.

In Fig.3, the colors fade from red to blue representing the gradual decay of potential from 5 V to 0 V. The cathode steel rods locate at the bottom where the potential is zero, and the anode carbon block on top of the cell provides the highest potential, 5V. It falls gradually in the electrolyte and slightly in the aluminum. Although the aluminum conductivity is significantly large, it's not iso-potential because of the huge current going through. The potential downward tendency appears a turning point just at the boundary layer.

4 Determination of the Boundary

4.1 Potential Distribution Detection

We developed an automatic measurement setup to detect the potential distribution vertically in the cell, which consists of a probe rod driven by a motor, a probe travel encoder, a potential acquisition unit and a minicomputer, partially referring to Fig.4.

Fig.4 Detect the Potential Distribution in an Aluminum Electrolytic Cell

4.2 Data Analysis

The potential changes during the probe rod descending and ascending, seeing Fig.5.

While initiating a measurement procedure, the probe rod descends in air step by step from the highest position A (Fig.3), and the potential maintains about zero, which is corresponding to the segment A~B in Fig.4. It will sharply arise once the probe rod contacts the electrolyte, seeing the cliff line at point B in Fig.5.

After that, the probe rod will insert into the molten electrolyte, and the potential will drop continuously in a certain rate until the boundary being

reached, seeing the segment B~C in Fig.5.

The boundary position is at a knee point C under where the potential will drop in a relatively small rate, which means the probe rod inserting into the molten aluminum layer, seeing the segment C~D.

When the maximum travel is approached, the probe rod will change direction and ascend step by step. The potential varies in opposite tendency, seeing the right side in Fig.5.

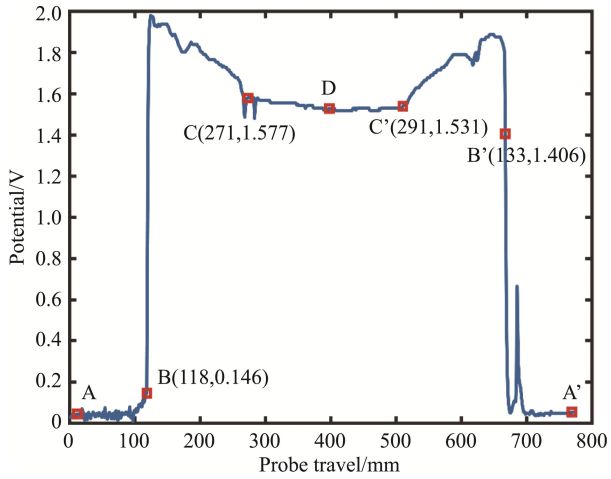

Fig.5 The Potential Distribution with Probe Rod Positions

4.3 Boundary Determination

In order to get the depth of the boundary, we should identify 2 knee points, the air-electrolyte interface point B and the electrolyte-aluminum interface point C. The distance between point B and C is the boundary depth.

Determination of point B: Let the probe rod descend step by step and monitor the differential potential at each step. The point B can be acknowledged if a preset threshold is reached.

Determination of point C: it's identified in the similar way except a relatively small threshold is adopted.

In fact, the measurement can be carried both in descending and ascending travel. Two groups of knee points B, C and B', C', or calculated depths 153mm and 158mm, are reasonable. We take their average, 156mm, as the final result.

We took measurements in three consecutive days, and the calculated boundary depths were 156mm, 178mm and 152mm. At the same time, carefully conducted manual measurements were 170mm, 160mm and 160mm. The differences are less than 5% which is acceptable in practice. The errors come from the viscous hanging along the probe rod. As shown in Table 2.

Table 2 Comparison of Manual and Automatic Measurements

	Date	Manual measurement	Automatic measurement	Difference
Depth of the boundary	Day1	170	178	4%
	Day2	160	156	2.5%
	Day3	160	152	5%

5 Conclusion

Through analyzing the electrochemical process conducted in aluminum production, and simulating the electric field distribution in electrolytic cells, we developed a technic to measure the electric potential automatically and determine the depth of boundary between molten electrolyte and aluminum. That's significant to substitute the poor efficiency and dangerous measurement work manually and is necessary to maintain efficient and optimal production.

References

[1] ZHANG Zhaohui, ZHAO Xiaoyan, BIAN Xinxiao, MAO Guanqiao, WANG Daohui, LU Hui, CAO Bin. (2019). Impedance measurements under strong magnetic interference around the aluminum electrolytic cells, Metallurgical Industry Automation. 43(4). pp.69-72.

[2] Wang, X., Peterson, R.D., Tabereaux, A.T. (2016). Electrical Conductivity of Cryolitic Melts, Essential Readings in Light Metals, Springer, Cham, 2016, pp. 57-64.

[3] Híveš, J., Thonstad, J., Sterten, Å. and Fellner, P. (1993). Electrical conductivity of molten cryolite-based mixtures obtained with a tube-type cell made of pyrolytic boron nitride, Metallurgical and Materials Transactions B, pp.255-261.

[4] Tabereaux, A.T., &Peterson, R.D. (2014). Aluminum Production. Treatise on Process Metallurgy, pp.839–917.

[5] S. Hudson, J. Craparo, R. De Saro, D. (2016). Laser-induced breakdown spectroscopy: a new tool for real time melt cognition, Metallurgia Italiana, pp. 5-8.

[6] Aroba Saleem, Peter Ross Underhill, David Chataway, Terry Gerritsen, Afshin Sadri, and Thomas W. Krause. (2020). Electromagnetic Measurement of Molten Metal Level in Pyrometallurgical Furnaces, IEEE Transactions on Instrumentation and Measurement, 69(6), pp. 3118-3125.

[7] S. Kolas, T. Store. (2009). Bath temperature and AlF3 control of an aluminum electrolysis cell, Control Engineering Practice, 17(9), pp. 1035-1043.

[8] Toshihiko Kiwa, Yohei Fukudome, Shingo Miyazaki, Mohd Mawardi Saari, Kenji Sakai, Akira Tsukamoto, Seiji Adachi, Keiichi Tanabe, Akihiko Kandori, Keiji Tsukada. (2013). Magnetic Detection of Currents in an Electrolytic Cell Using High-TC Squid, IEEE Trans. on Applied Superconductivity, 23(3), pp. 1600804-1600804.

[9] Wei Liu. (2010). Mathematical Modeling of Mul-tiple Physical Fields and Its Application in Aluminum Reduction Cells. Central South University.

[10] Jie Li, Hongliang Zhang, Yujie Xu. (2011). Simulated computation and optimization of comprehensive physical fields in modern large-scale aluminum reduction cells, The Chinese Journal of Nonferrous Metals, 21(10), pp 2594-2606.

[11] Jia Zhang. (2018) Simulation of thermal field of a 500KA electrolytic cell in an electrolytic aluminum plant, Nonferrous Metals Engineering & Research, 39(3), pp.51-54.

Author Biographies

CHANG Liming is currently a M.Sc. candidate in School of Automation and Electrical Engineering, University of Science and Technology Beijing. His main research interests include industrial sensors and embedded instruments.

E-mail: dawn9617@163.com

ZHANG Zhaohui received Ph.D. degree from Southeast University in 1999. He is currently a professor in University of Science and Technology Beijing. His main research interest includes intelligent instrumentation and terahertz detection.

E-mail: zhangzhaohui@ustb.edu.cn

ZHAO Xiaoyan received her Ph.D. degree from University of Science and Technology Beijing in 2009. She is currently an associate professor in the University. Her main research interest includes the intelligent instrumentation.

ZUO Zengyang is currently a M.Sc. candidate in School of Automation and Electrical Engineering, University of Science and Technology Beijing. His main research interest includes the intelligent instrumentation.

LU Hui received his Ph.D. from University of Science and Technology Beijing in 2022. He currently works in Guiyang Aluminum Magnesium Design Institute Co., Ltd.

LAO Dabao received his Ph.D. from Tianjin University in 2011. He is currently an associate professor. His main research interests include the research of optoelectronic large-size measurement technology and instrumentation.